Journal of Applied Physics

RESEARCH ARTICLE | OCTOBER 11 2010

# Impedance spectroscopy of $BaTiO_3$ cubes suspended in lossy liquids as a physical model of two-phase system

Piotr Jasinski; Vladimir Petrovsky; Fatih Dogan



*J. Appl. Phys.* 108, 074111 (2010)
https://doi.org/10.1063/1.3486461







AIP Publishing

# Impedance spectroscopy of $BaTiO_3$ cubes suspended in lossy liquids as a physical model of two-phase system

Piotr Jasinski,[1,2,a)] Vladimir Petrovsky,[1] and Fatih Dogan[1]
[1]*Department of Materials Science and Engineering, Missouri University of Science and Technology, Rolla, Missouri 65409, USA*
[2]*Faculty of Electronics, Telecommunications and Informatics, Gdansk University of Technology, Gdansk 80-233, Poland*

(Received 10 March 2010; accepted 7 August 2010; published online 11 October 2010)

Impedance spectroscopy techniques were used for analysis of the physical model in a two-phase system toward determining of dielectric constant of dielectric particles suspended in liquids at various solids loading (volume fraction) levels. Model experimental studies were conducted using $BaTiO_3$ as a dielectric material that was prepared as small cubes of uniform size ($2\times2\times1$ mm). Barium titanate (BT) cubes having a dielectric constant of 3850 were immersed in liquids of low dielectric constant and moderate electrical conductivity. Measured impedance spectra consisted of two semicircles, which were fitted for (R‖C)(R‖C) equivalent circuit. The parameters obtained from fitting were compared with the data acquired from simulations of brick layer models and Maxwell–Wagner effective media model. In the investigated range of volume fractions the Maxwell–Wagner model correlates well with the data extracted from measurements. © *2010 American Institute of Physics*. [doi:10.1063/1.3486461]

## I. INTRODUCTION

Impedance spectroscopy is a powerful tool used to investigate electrical properties of electroceramics. It provides insight on, e.g., grain and grain boundary conductivity,[1,2] diffusion processes,[3,4] mixed conducting transport properties,[5] and electrochemical reactions[6,7] in various materials. It has been previously used to investigate two-phase systems.[8–10] However, this technique is commonly used to analyze the systems, in which the individual components were undefined due to the complex nature of these systems. For example, in case of polycrystalline ceramics, volume fraction and dielectric constant of grain boundaries and shape of the grains are unknown or difficult to define.[11,12] It becomes challenging to compare the experimental results with predictions of mathematical models describing two-phase systems, since these models assume fixed parameters such as standard size, shape, and periodic distribution of inclusions.

We have been using previously impedance spectroscopy to determine dielectric properties of two-phase systems. Namely, it was used to calculate dielectric constant of powders suspended in lossy liquids.[13–17] It seems to be exceptional method to provide information about dielectric constant of powders for the purpose of composite capacitor fabrication (e.g., polymer–ceramic) or quality assurance during dielectric powders fabrication. In this method, the dielectric constant is calculated from low frequency semicircle of the spectra obtained from powders dispersed in lossy liquids.[17] Although, the method has been proven on variety of different powders[15] but so far there was lack of model, which would describe complex nature of the results obtained using this method. For example, an increase in calculated dielectric constant for low volume fractions of powders.[17] This paper intends to provide a mathematical model, which could be used to describe obtained results.

We believe that there is the gap in complexity between real two-phase systems and mathematical models used for its description. Physical modeling could be effective approach for solving this problem. Therefore, the main objective of this work was to prepare a well defined experimental model structure of a two-phase system and to compare the impedance spectra of these structures with the impedance spectra generated mathematically by different theoretical models of two-phase systems.

## II. EXPERIMENTAL

Impedance spectroscopic measurements of two-phase system were conducted using barium titanate (BT) cubes uniformly distributed in a lossy liquid as described elsewhere.[16] Figure 1 shows two types of equipotential surfaces perpendicular to the electrical field and two types of surfaces of uniform electric field parallel to the electrical field. One type of these surfaces is located half distance between the cubes, while the other in the middle of cubes. The surfaces marked in the picture create periodic structures. In this way an elementary cell of the structure (used for equivalent circuit modeling) and a concept of measurement setup (fixture) can be depicted. In case of the measurement fixture, the distance between electrodes should be as small as possible, so the ratio of area of electrodes and distance between electrodes could be as large as possible. This allows suppressing edge effects. Additionally, it is not practical (possible) to suspend cubes in liquid in all three dimensions. Therefore, the structures with only one half-period localized between the two equipotential surfaces are used for measurements. As a consequence, the cubes needs to be half in height

a)Electronic mail: Piotr.Jasinski@eti.pg.gda.pl.

 

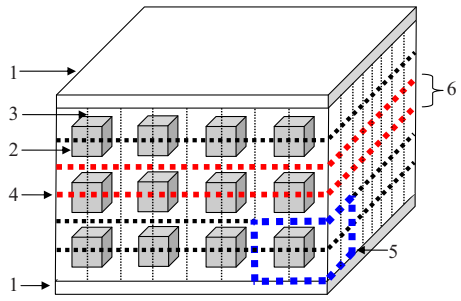


FIG. 1. (Color online) Schematic representation of ceramic cubes suspended in liquid in the presence of electrical field: 1—electrodes, 2—ceramic cubes, 3—uniform electric field lines forming perpendicular surfaces to electrode surfaces, 4—equipotential surfaces parallel to electrode surfaces, 5—elementary cell of brick layer model, and 6—part of brick layer structure limited by equipotential surfaces used as a concept of experimental fixture (see Fig. 2).

(i.e., the cube geometry should be $a \times a \times (a/2)$) and the distance between the electrodes should be half of the distance between the cubes. Following these assumptions, a physical model of two-phase system was developed and described in detail.

BT cubes were prepared using X7R422H powder (Ferro, Cleveland, Ohio, USA). The powder was uniaxially pressed in the stainless steel die to form cylindrical compacts followed by isostatic pressing at 300 MPa. The compacts were sintered at 1300 °C for 2 h and cut into cubes of $2 \times 2 \times 1$ mm using a diamond saw. In order to obtain dielectric constant of ceramic material the disks of 17 mm in diameter and 1 mm thick were prepared. Silver paint was applied to form metallic electrodes. The dielectric constant of 3850 was obtained.

Dielectric measurements of BT cubes in lossy liquids were performed in a cell, which cross-section is schematically presented in Fig. 2. The cell consists of two graphite electrodes separated by alumina spacers. A graphite plate (GR-940, Graphtek LLC, USA) was used as electrode material. The bottom electrode was partially encapsulated in epoxy in order to fix the size of conductive surface that can be used for placement of the cubes. The top electrode was not coated with epoxy and had a larger surface area than that of the bottom electrode. The distance between top and bottom electrodes was fixed by alumina spacers placed on epoxy part of electrode. The height of spacers was adjusted to fit the requirement of the model, i.e., the spacer height is half of the distance between the cubes. Namely, the height of the spacer $s$ was fixed using Eq. (1)

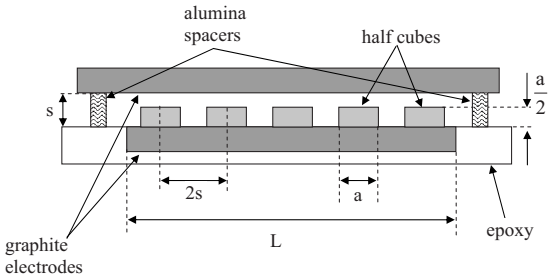


FIG. 2. Cross section of measurement cell.

$$s = \frac{L}{2\sqrt{N}}, \tag{1}$$

where $L$ is the length of the electrode side and $N$ is the number of the cubes.

It was intended to perform measurements for the wide range of volume fractions. It is straightforward to derive relation between the volume fraction $X$, the length of electrode size $L$, and the number of cubes $N$, as follows in Eq. (2):

$$X = \frac{Na^3}{2sL^2}, \tag{2}$$

where $a$ is the length of cube side.

By substituting Eq. (1) into Eq. (2) one may obtain following Eq. (3):

$$X = \left(\frac{\sqrt{N}a}{L}\right)^3. \tag{3}$$

Since the size of cubes $a$ is fixed, one may obtain wide range of different volume fractions by altering the number of the cubes or by altering the area of the electrodes. Both methods were used to obtain different volume fraction. Although, theoretically speaking, one cube is enough to perform measurements but measurement uncertainties due to edge effects and other errors could be significant. If large number of cubes is used for measurements then those uncertainties are minimized but electrodes with large surface areas need to be employed. As a compromise, at first approach, the numbers of cubes was fixed at 36, whereas the results obtained using this configuration are referred as "$6 \times 6$." In a consequence electrodes with various surface areas (1.67 to 31 $cm^2$) were fabricated and used for these measurements. The "$6 \times 6$" configuration allowed covering volume fraction range from 0.75 to 0.01.

In case of the "$6 \times 6$" configuration the number of cubes is constant and, it is expected, that the measurement uncertainties should be the similar for each volume fraction. To evaluate this effect, as a second approach, the number of cubes was increased (up to 169), while the size of the electrodes was fixed (10.6 $cm^2$). As a result it was possible to obtain the volume fractions range from 0.5 to 0.05. The corresponded results were referred as "$A \times A$." Additionally, to obtain more accurate values of the volume fraction, each set of cubes was weighed before the measurements and the volume fraction was adjusted using following Eq. (4):

$$X = \frac{m}{dsL^2}, \tag{4}$$

where $m$ is the weight of cubes and $d$ is the density of BT.

The table listing of all experimental details related to the "$6 \times 6$" and "$A \times A$" configurations are presented in Table I and Table II, respectively. The measurements were performed in butoxyethanol (BOE) (Aldrich, USA) and propylene carbonate (PC) (Aldrich, USA).

The impedance spectra were collected in a frequency range from 1 Hz to 1 MHz with an applied voltage of 20 mV

TABLE I. Experimental details of "6×6" configuration.

| No. of cubes $N$ | Volume fraction | Electrode side length $L$ (cm) | Electrode area $L^2$ (cm$^2$) | Spacer $s$ (mm) |
|---|---|---|---|---|
| 36 | 0.74 | 1.29 | 1.67 | 1.07 |
| 36 | 0.55 | 1.42 | 2.02 | 1.18 |
| 36 | 0.46 | 1.51 | 2.29 | 1.26 |
| 36 | 0.29 | 1.79 | 3.21 | 1.49 |
| 36 | 0.19 | 2.05 | 4.21 | 1.71 |
| 36 | 0.10 | 2.59 | 6.68 | 2.15 |
| 36 | 0.05 | 3.26 | 10.61 | 2.71 |
| 36 | 0.02 | 4.42 | 19.54 | 3.68 |
| 36 | 0.01 | 5.57 | 31.01 | 4.64 |

TABLE II. Experimental details of "A×A" configuration.

| No. of cubes $N$ | Volume fraction | Electrode side length $L$ (cm) | Electrode area $L^2$ (cm$^2$) | Spacer $s$ (mm) |
|---|---|---|---|---|
| 36 | 0.05 | 3.26 | 10.61 | 2.71 |
| 64 | 0.11 | 3.26 | 10.61 | 2.03 |
| 81 | 0.16 | 3.26 | 10.61 | 1.81 |
| 100 | 0.23 | 3.26 | 10.61 | 1.62 |
| 121 | 0.30 | 3.26 | 10.61 | 1.48 |
| 169 | 0.49 | 3.26 | 10.61 | 1.25 |

using a Solartron 1260 frequency response analyzer connected to a Solartron 1296 Dielectric Interface (Ametek, USA).

## III. EQUIVALENT CIRCUIT AND EFFECTIVE MEDIUM MAXWELL-WAGNER MODELS

Mathematical equivalent of the physical structure described in previous section is a Brick Layer Model, which is frequently used to describe electrical properties of polycrystalline ceramics.[18,19] The model contains all basic features of the physical structure used for experimental measurements; periodic distribution of oriented cubic inclusions. However, a direct analytical solution of impedance spectra for this model cannot be obtained, since the electrical field has a complex three-dimensional (3D) distribution. Finite-difference computer algorithms need to be employed to calculate the impedance spectra. Such algorithms, referred as "nested-cube" or "3D brick layer,"[8,11] consider a 3D distribution of the electrical field. However, in this approach closed-form solution does not exist and the problem must be solved numerically for each particular structure parameter.[11] Hence, these methods were not considered in this study.

The simplest models used to describe the electrical properties of two-phase mixtures are the "series layer model" and the "parallel layer model."[19] They use a two-area structure to describe electrical properties of the mixture, i.e., each phase associated with one area. Those models illustrate two extreme cases, where both or neither of the phases are continuous.[19] In each area electrical field is uniform, which allows transition to equivalent circuits. These equivalent circuits provide limits for any real two-phase system; however, those limits are very wide.

The brick layer model approach allows narrow those limits. An electrical field is not uniform in the elementary cell of brick layer model but the elementary cell can be divided onto three-area structures with the uniform field distribution in each area. Only two such structures can be built and consequently two related equivalent circuit can be formed as depicted in Figs. 3 and 4, respectively. These models are not exact approximation of a real system, since they assume parallel flow of current without distortion around edges,[18] but they will provide much better approximation of two-phase system, than the two-area structures. They will also provide upper and lower limits for their impedance/dielectric response of periodically distributed cubes in lossy liquid. Therefore, one may expect that parameters extracted from experimentally measured impedance spectra should fall between parameters extracted from both models. Note, that model 2 is equivalent to series-parallel brick layer model (SP-BLM) (Refs. 8 and 11) and brick layer model (BLM) (Ref. 12) models.

Figures 3 and 4 show corresponding equivalent circuits and equations as a function of volume fraction and properties of each phase. Note, that the elements of equivalent circuit are denoted as resistance and capacitance but they indeed represent resistivity (in ohm meter) and absolute permittivity (farad per meter), respectively; while geometry of the model cell is assumed to be unity (1 m$^3$). The elements of equivalent circuit can be used to calculate impedance of models in order to simulate impedance spectra. For model 1 and model 2 the impedance can be schematically described by Eqs. (5) and (6), respectively,

$$Z_{(R_1\|C_1\|C_D)\circ(R_2\|C_2)} = f(\rho_h, \varepsilon_h, \varepsilon_i, X, \omega), \tag{5}$$

$$Z_{[(R_2\|C_2)\circ C_D]\|R_1\|C_1} = f(\rho_h, \varepsilon_h, \varepsilon_i, X, \omega), \tag{6}$$

where ‖ represents parallel connection of two elements, while ∘ series, $\varepsilon_i$—dielectric constant of inclusion (ceramic cube), $\varepsilon_h$—dielectric constant of host (liquid), $\rho_h$—resistivity of host (liquid), $X$—volume fraction, and $\omega$—angular frequency.

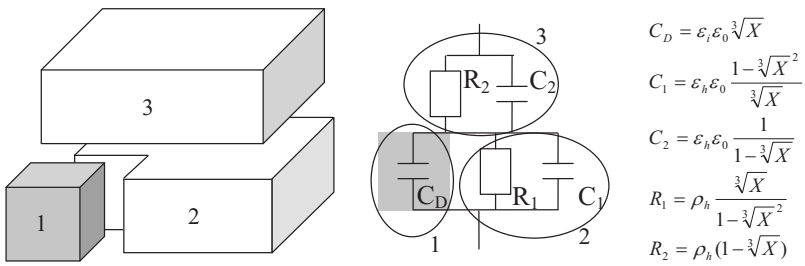


FIG. 3. Model 1: schematic representation of cube suspended in liquid (a), equivalent circuit (b), and values of each element as a function of volume fraction $X$ (c) [$\varepsilon_o$—the dielectric constant of vacuum, $\varepsilon_i$—dielectric constant of inclusion (ceramic cube), $\varepsilon_h$—dielectric constant of host (lossy liquid), $\rho_h$—resistivity of host (lossy liquid)].

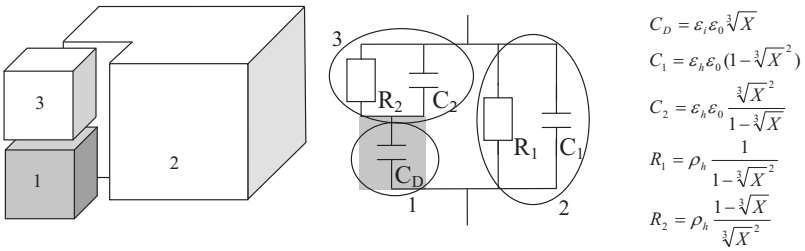


FIG. 4. Model 2: schematic representation of cube suspended in liquid (a), equivalent circuit (b), and values of each element as a function of volume fraction (c) [$\varepsilon_o$—the dielectric constant of vacuum, $\varepsilon_i$—dielectric constant of inclusion (ceramic cube), $\varepsilon_h$—dielectric constant of host (lossy liquid), and $\rho_h$—resistivity of host (lossy liquid)].

Among the various effective media theories, the Maxwell–Wagner model was selected for comparison with experimental data. It was found that expansion of Maxwell–Wagner model on complex conductivities allows describing impedance spectra of two-phase composite systems such as grain and grain boundary in ceramics with controlled grain size.[11] The Maxwell–Wagner model is described by equation as follows:[7,18]

$$\frac{(\sigma_e - j\omega\varepsilon_0\varepsilon_e) - (\sigma_h - j\omega\varepsilon_0\varepsilon_h)}{(\sigma_e - j\omega\varepsilon_0\varepsilon_e) + 2(\sigma_h - j\omega\varepsilon_0\varepsilon_h)} = X\frac{-j\omega\varepsilon_0\varepsilon_i - (\sigma_h - j\omega\varepsilon_0\varepsilon_h)}{-j\omega\varepsilon_0\varepsilon_i + 2(\sigma_h - j\omega\varepsilon_0\varepsilon_h)}, \quad (7)$$

where $\varepsilon_e$—effective dielectric constant of two-phase system, $\sigma_e$—effective conductivity of two-phase system, $\varepsilon_i$—dielectric constant of inclusion (ceramic cube), $\varepsilon_h$—dielectric constant of host (liquid), $\sigma_h$—conductivity of host (liquid), $X$—volume fraction, $\omega$—angular frequency, $j$—the imaginary unit, and $\varepsilon_0$—dielectric constant of vacuum.

Expression for impedance may be obtained using following Eq. (8):

$$Z = \frac{1}{Y} = \frac{1}{\sigma_e - j\omega\varepsilon_0\varepsilon_e} = \frac{\sigma_e}{\sigma_e^2 + (\omega\varepsilon_0\varepsilon_e)^2} + j\frac{\omega\varepsilon_0\varepsilon_e}{\sigma_e^2 + (\omega\varepsilon_0\varepsilon_e)^2} = f(\sigma_h, \varepsilon_h, \varepsilon_i, X, \omega), \quad (8)$$

and can be used to simulate impedance spectra, what will be described below in detail.

## IV. DATA ANALYSIS

The flowchart for data analysis is shown in Fig. 5. The impedance spectra were obtained from measurement of periodically distributed ceramic cubes in BOE and PC and from computer simulation based on equivalent circuit and Maxwell–Wagner models. The spectra were then fitted using ZVIEW software (Scribner, USA) to an equivalent circuit. The procedure of data analysis is described in the following.

As an example, a typical impedance spectrum is presented in Fig. 6 (volume fraction 0.19, cubes distribution 6 × 6). The spectra always consist of two semicircles and a tail at low frequencies. The low frequency tail is related to the double layer capacitance of the electrodes and is not of interest here. For identification, the loops are referred as high and low frequency semicircles. The equivalent circuit, which is utilized for fitting of data, is shown in Fig. 5. It consists of high and low frequency relaxation connected is series. Capacitance $C_{HF}$ and resistance $R_{HF}$ are attributed to high frequency semicircle, while the constant phase element $\text{CPE}_{LF}$ and resistance $R_{LF}$ to low frequency semicircle. It is necessary to use the CPEs in the equivalent circuit since the low frequency semicircle is slightly depressed. The impedance of CPE is described by following Eq. (9):

$$Z_{\text{CPE}} = \frac{1}{Q(j\omega)^n}, \quad (9)$$

where $Q$ and $n$ are the parameters of CPE, $j$ the imaginary unit, and $\omega$ the angular frequency. In order to calculate capacitance of low frequency relaxation process, parameters of the CPE ($Q_{LF}, n_{LF}$) and resistance $R_{LF}$ need to be used in the following Eq. (10):[11,20]

$$C_{LF} = (Q_{LF})^{1/n_{LF}} (R_{LF})^{1 - n_{LF}/n_{LF}}. \quad (10)$$

Knowing the capacitances attributed to low and high frequency semicircles the corresponding dielectric constants can be calculated using following Eqs. (11) and (12):

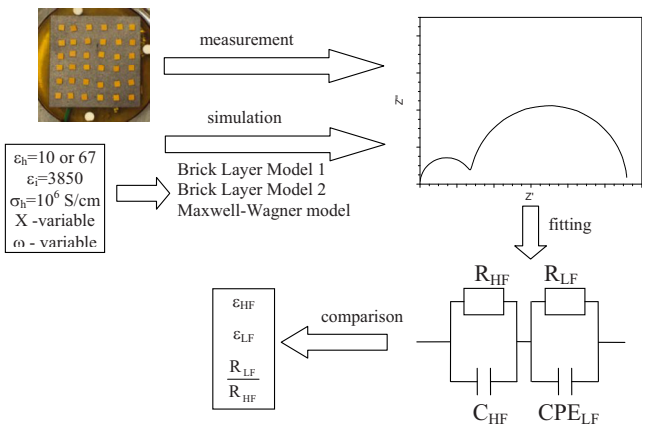


FIG. 5. (Color online) Data analysis procedure.

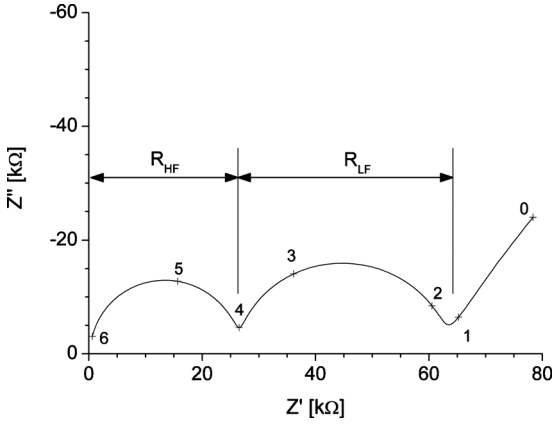


FIG. 6. Typical impedance spectra of cubes suspended in BOE. Solid fraction 0.19, distribution 6 × 6. The numbers reflect exponent of frequency.

TABLE III. Data obtained from fitting of impedance spectra presented in Fig. 5 and Eqs. (10)–(12).

| High frequency semicircle | | Low frequency semicircle | | |
|---|---|---|---|---|
| $C_{HF}$=49.5 pF | $R_{HF}$=25.6 kΩ | $R_{LF}$=37.1 kΩ | $Q_{LF}$=20.5×10$^{-9}$ s$^{0.89}$/Ω | $n_{LF}$=0.89 |
| | | | $C_{LF}$=8.4 nF | |
| $\varepsilon_{HF}$=17.4 | | $R_{LF}/R_{HF}$=1.23 | $\varepsilon_{LF}$=3850 | |

$$\varepsilon_{HF} = \frac{C_{HF}}{\varepsilon_o}\frac{s}{L^2}, \tag{11}$$

$$\varepsilon_{LF} = \frac{C_{LF}}{\varepsilon_o}\frac{s}{L^2}, \tag{12}$$

where $\varepsilon_o$ is the dielectric constant of vacuum, $s$ the distance between the electrodes of electrochemical cell, and $L^2$ the electrode surface area.

As an example, the data obtained from fitting of impedance spectra presented in Fig. 6 and calculated using Eqs. (10)–(12) are shown in Table III.

Impedance spectra were simulated for models 1 and 2 and Maxwell–Wagner effective media model for different volume fractions. In calculations, actual values of the dielectric constant of liquid and ceramics cubes ($\varepsilon_h$=10 for BOE, $\varepsilon_h$=67 for PC, and $\varepsilon_i$=3850 for ceramic cubes) were used. Conductivity of the liquid was assumed to be $\sigma_h$ =10$^{-6}$ S/cm, that was close to the actual value. The exact value of conductivity was not necessary for comparison purposes. For each model, the simulated impedance spectra contain two semicircles. The simulated impedance spectra were analyzed using the same procedure to obtain parameters $\varepsilon_{HF}$, $\varepsilon_{LF}$, and $R_{LF}/R_{HF}$ as it was described for experimental data.

Direct comparison of impedance spectra obtained from measurements and simulations using Maxwell–Wagner model for volume fraction $X$=0.3 is presented in Fig. 7. In this case, the conductivity of liquid ($\sigma_h$=1.4×10$^{-6}$ S/cm) was used in the Maxwell–Wagner simulation. It is shown that, in comparison to experimental data, the low frequency semicircle obtained for Maxwell–Wagner model is not depressed. Indeed, for Maxwell–Wagner model and for model 1 and 2 the CPE exponential factor $n_{LF}$ was always $n_{LF}$=1 and therefore one could use a capacitance instead of CPE in equivalent circuit. The depression of low frequency semicircle in experimental data can be attributed to nonuniform field distribution in the brick layer structure. Additionally, the cubes are not exactly the same in size and shape, which could also lead to distribution of value of the equivalent circuit elements. Note, that in case of the model 1 the parameters $R_{HF}$, $C_{HF}$, $R_{LF}$, and $C_{LF}$ can be obtained without simulation of impedance spectra and fitting to equivalent circuit presented in Fig. 5. This is possible, because the equivalent circuit presented in Fig. 3 is equivalent to the circuit in Fig. 5 using following substitutions: $R_{HF}=R_2$, $C_{HF}=C_2$, $R_{LF}=R_1$, and $C_{LF}=C_1+C_D$. In case of the Maxwell–Wagner model the parameters $R_{HF}$, $C_{HF}$, $R_{LF}$, and $C_{LF}$ can alternatively be obtained using so called Bonanos–Lilley set of equations.[21]

## V. RESULTS AND DISCUSSION

Impedance spectroscopy measurements of ceramic cubes suspended in a lossy liquid were performed for different volume fractions (from 0.75 to 0.01) of cubes with different distributions pattern (6×6 and A×A) and two types of liquids (BOE and PC). The parameters $R_{LF}/R_{HF}$, $\varepsilon_{HF}$, and $\varepsilon_{LF}$ were extracted from spectra and are presented as a function of volume fraction in Figs. 8–10, respectively. Along with experimental results, the data extracted from simulated spectra are plotted. The parameters extracted from measurements are marked using symbols while from the simulation are represented by continuous lines.

Figure 8 shows the ratio of resistances related to low and high frequency semicircle [simulated spectra are only for one type of liquid (BOE)]. The data obtained from simulations of all models are in agreement with the data obtained from measurements. Particularly, Maxwell–Wagner model and

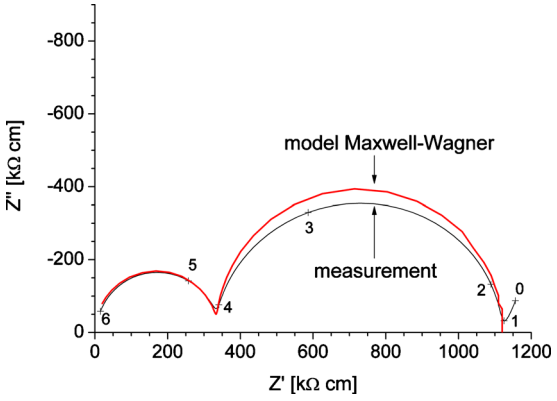


FIG. 7. (Color online) Impedance spectra of cubes suspended in BOE and the spectrum simulated using Maxwell–Wagner model. Volume fraction of solid $X$=0.29, distribution 6×6. In case of Maxwell–Wagner mode $\varepsilon_i$ =3850, $\varepsilon_h$=10, and $\sigma_h$=1.4×10$^{-6}$ S/cm. The numbers reflect exponent of frequency.

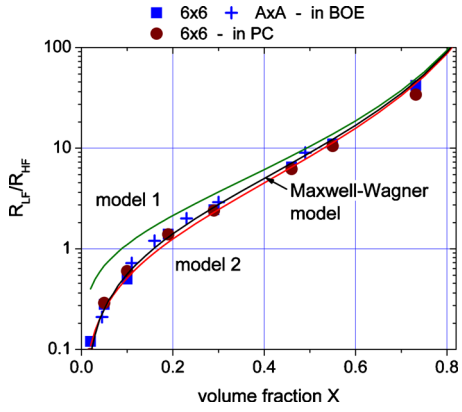


FIG. 8. (Color online) Ratio of resistances connected, respectively, to low and high frequency semicircles as a function of volume fraction of ceramic cubes. In case of the parameters obtained from simulated impedance spectra: $\varepsilon_h$=10, $\varepsilon_i$=3850, and $\rho_h$=10$^6$ Ω cm.

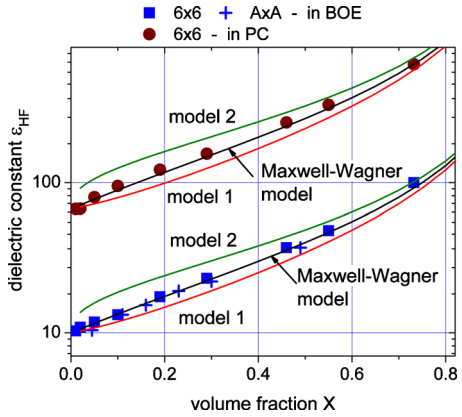


FIG. 9. (Color online) Dielectric constant calculated from the capacitance connected to high frequency semicircle as a function of volume fraction of ceramic cubes. In case of the parameters obtained from simulated impedance spectra: $\varepsilon_h=10$ for BOE, $\varepsilon_h=67$ for PC, and $\varepsilon_i=3850$, $\rho_h=10^6$ Ω cm.

equivalent circuit model 2 reproduce the results obtained from measurements. Different type of host liquids (PC and BOE) with differences in their dielectric constant and conductivity, do not influence the ratio of $R_{LF}/R_{HF}$. It is related to fact that there is only one source for both high and low frequency resistances (i.e., resistivity of liquid) which explains stability of the ratio $R_{LF}/R_{HF}$ and its independence on type of host liquid. This fact was confirmed in details in our previous publication.[13] The independence of resistances ratio from liquid conductivity is also confirmed by simulation of impedance spectra using equivalent circuit model 1 and model 2. In both cases the ratio of resistance in not influenced by conductivity level. It is related to fact that the resistances always reversely proportional to the conductivity of liquid and therefore in the form of ratio the conductivity is reduced from the fraction. In case of the BOE, distribution pattern of cubes (6×6 or A×A) does not affect the obtained results of $R_{LF}/R_{HF}$.

The dielectric constant ($\varepsilon_{HF}$) calculated from the capacitance connected to the high frequency semicircle ($C_{HF}$) as a function of volume fraction of ceramic cubes is presented in Fig. 9. It is shown that for each type of liquid distinct data sets similar in trend are obtained. For the same volume fraction the dielectric constant $\varepsilon_{HF}$ for PC is always higher than for BOE, which is in agreement with the fact that dielectric constant of PC is about seven times larger than of BOE. The data obtained for each liquid from simulated impedance spectra based on the equivalent circuit model 1 and 2 provide narrow limits for parameters obtained from measurements and from Maxwell–Wagner model. The parameters obtained from Maxwell–Wagner model, within experimental error, follow the parameters obtained from measurements. The distribution pattern of cubes (6×6 or A×A) does not influence obtained results.

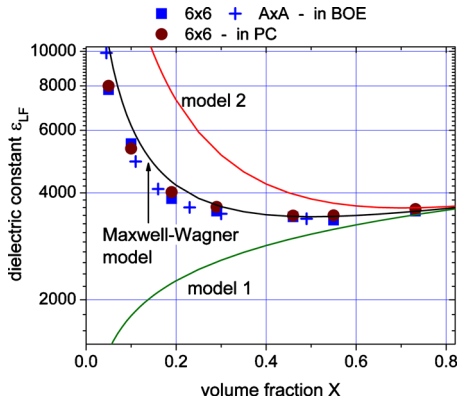


FIG. 10. (Color online) Dielectric constant calculated from the capacitance connected to low frequency semicircle as a function of volume fraction of ceramic cubes. In case of the parameters obtained from simulated impedance spectra: $\varepsilon_h=10$, $\varepsilon_i=3850$, and $\rho_h=10^6$ Ω cm.

The dielectric constant $\varepsilon_{LF}$ calculated from the CPE connected to the low frequency semicircle ($CPE_{LF}$) as a function of volume fraction of ceramic cubes is presented in Fig. 10. The simulated spectra, which were used to obtain dielectric constant $\varepsilon_{LF}$, were generated only for $\varepsilon_h=10$ (BOE), because $\varepsilon_{LF}$ is not significantly sensitive to variations in $\varepsilon_h$. It is also confirmed by the data obtained from measurements, i.e., within experimental accuracy the same values of $\varepsilon_{LF}$ were obtained for PC and BOE. In case of BOE, distribution pattern of cubes (6×6 or A×A) does not influence obtained results. Similar to $C_{HF}$, data obtained from measurements are limited by parameters obtained from equivalent circuit models. For volume fractions $X<0.4$ the difference between the data obtained from equivalent circuit models and from measurements become large. Data extracted from simulated impedance spectra using Maxwell–Wagner model follow data acquired from measurements. For the low volume fraction $X<0.25$ data obtained from measurements are slightly lower than that from Maxwell–Wagner model. However, the trend is very similar.

It can be concluded that, as it was expected, parameters obtained from simulated impedance spectra using equivalent circuit models provide the limits for experimental data. This is also true even in case of very narrow bounds ($R_{LF}/R_{HF}$ and $\varepsilon_{HF}$). The parameters are not sensitive to distribution pattern of cubes. The $R_{LF}/R_{HF}$ and $\varepsilon_{LF}$ are not altered by the dielectric constant of host liquid and its conductivity. The effective media Maxwell–Wagner model is in a good agreement with the data obtained from measurements. Only very slight deviation between data obtained from measurements and from Maxwell–Wagner model exists in case of the $\varepsilon_{LF}$ for small volume fractions. The possible reason for this deviation is described below.

It should be noted, that the solid lines in Figs. 8–10 related to Maxwell–Wagner model were not an approximation of experimental data but simulation for given experimental conditions. One may expect that the dielectric constants and the volume fractions of ceramic cubes were obtained with limited accuracy. To estimate the origin of this error, sensitivity of parameters $R_{LF}/R_{HF}$, $\varepsilon_{HF}$, and $\varepsilon_{LF}$ on limited accuracy of dielectric constants of liquid and ceramic cubes and volume fractions were calculated and presented in Table IV and Table V, respectively. It was assumed, that maximum 5% of relative inaccuracy could be expected for input parameters $\varepsilon_h$, $\varepsilon_i$, and $X$.

If dielectric constants $\varepsilon_h$ and $\varepsilon_i$ are estimated inaccurately, (Table IV) a systematic error can affect the dielectric constants $\varepsilon_{HF}$ and $\varepsilon_{LF}$, respectively. The error level is inde-

TABLE IV. Sensitivity of dielectric constants $\varepsilon_{HF}$, $\varepsilon_{LF}$ calculated from Maxwell–Wagner model to 5% inaccuracy of input parameters (volume fraction $X=0.2$).

| Parameters | $\varepsilon_h=10\pm5\%$ | $\varepsilon_i=3850\pm5\%$ |
|---|---|---|
| $\varepsilon_{HF}=$ | $17.5\pm5\%$ | $17.5\pm0\%$ |
| $\varepsilon_{LF}=$ | $4205\pm0.01\%$ | $4205\pm4.99\%$ |

pendent from volume fraction $X$ and it is similar in value to initial inaccuracy. There is only slight correlation between $\varepsilon_h$ and $\varepsilon_{LF}$. It is less likely that such inaccuracy is present in this study, because it would introduce the same error both at high and at low volume fractions. As can be seen in case of the $\varepsilon_{LF}$ (see Fig. 9), the experimental data better reflects simulated results obtained using the Maxwell–Wagner model at high volume fractions than at low volume fractions.

If the volume fraction is estimated inaccurately the effect is more complicated. The inaccuracy can introduce different values of error for each parameter, different errors at different volume fractions and different errors if volume fraction is overestimated or underestimated. For the purpose of simplicity, only the case of the underestimation of volume fraction is shown in Table V. Largest errors were obtained for $\varepsilon_{HF}$ and $R_{LF}/R_{HF}$ at high volume fractions. For example, a 5% underestimation of volume fraction at $X=0.8$ will result in minus 34% of relative error for the $\varepsilon_{HF}$ and minus 19% for the $R_{LF}/R_{HF}$. Therefore, it is unlikely, that the deviations at low volume fraction for $\varepsilon_{LF}$ (Fig. 10) could be explained by inaccuracy of volume fraction, since for the highest calculated errors ($\varepsilon_{HF}$ and $R_{LF}/R_{HF}$) the difference between data obtained from experimental, and from simulation using the Maxwell–Wagner model is not noticeable.

Another possible reason, which could explain why parameters obtained from experimental data slightly deviate from the Maxwell–Wagner model, is the shape of investigated inclusions.[22,23] The Maxwell–Wagner model was developed for inclusions spherical in shape,[11] while the shape of inclusions investigated here is cubic. However, understanding the role of the shape factor require further studies.

In previous studies, impedance spectroscopy techniques were utilized to obtain information about dielectric constant of powders based on low frequency semicircle.[13–17] Up to now, there was lack of model, which would explain complicated nature of the parameters obtained form the spectra. The two-phase system investigated in this study may be considered as equivalent to suspended powders. As a consequence, Maxwell–Wagner model may provide background that could be used to explain the results obtained for the suspended powders. For example, the increase in dielectric constant obtained from low frequency semicircle at low volume fraction for the powders suspended in lossy liquids is similar in trend to $\varepsilon_{LF}$ presented in this investigation. However, additional studies are necessary to investigate applicability of Maxwell–Wagner model to powders suspended in lossy liquids. Most likely, this model needs to be modified since for inclusions spherical in shape, what is expected for powders, a percolation threshold occurs at inclusion volume fraction of 0.52 instead of 1.[8]

TABLE V. Sensitivity of dielectric constants $\varepsilon_{HF}$, $\varepsilon_{LF}$ and ratio of resistances $R_{LF}/R_{HF}$ calculated from Maxwell–Wagner model to 5% underestimation of volume fraction ($\varepsilon_h=10$, $\varepsilon_i=3850$).

| Parameters | $X=0.05-5\%$ | $X=0.2-5\%$ | $X=0.8-5\%$ |
|---|---|---|---|
| $\varepsilon_{HF}=$ | 11.6−0.72% | 17.5−2.6% | 130−19% |
| $\varepsilon_{LF}=$ | 10400+4.8% | 4205+2.3% | 3616−1.1% |
| $R_{LF}/R_{HF}=$ | 0.25−5.5% | 1.41−7.3% | 90−34% |

## VI. SUMMARY

Two-phase systems were investigated, for which the shape of inclusions, dielectric constants, conductivity, and volume fraction of each component were defined. Impedance spectroscopy techniques were utilized to investigate two-phase systems. The parameters obtained from fitting of experimental data to the equivalent circuit with two relaxation processes were compared with parameters obtained from simulated spectra. Simulated spectra were acquired based on two equivalent circuit approximations by following of Brick Layer and effective media Maxwell–Wagner models.

Based on data extracted from impedance spectra obtained for a wide range of volume fractions it can be stated, that the parameters $R_{LF}/R_{HF}$, $\varepsilon_{HF}$, and $\varepsilon_{LF}$ are independent of distribution pattern of cubes. It was shown, that $\varepsilon_{LF}$ is virtually independent of type of host liquid. As expected, the parameters $R_{LF}/R_{HF}$, $\varepsilon_{HF}$, and $\varepsilon_{LF}$ obtained from measurements are within the limits provided by the equivalent circuit approximations. In the investigated range of volume fractions, the parameters obtained from measurements are similar in value to those from simulations using Maxwell–Wagner model. The slight deviations for $\varepsilon_{LF}$ in low volume fractions could probably be assigned to the shape of the second phase (spherical in the model in comparison to cubic in experimental setup). However, this hypothesis requires further confirmation.

## ACKNOWLEDGMENTS

Authors would like to thank Dr. Eugene Furman for fruitful discussion. This work was supported a MURI program sponsored by Office of Naval Research under Grant No. N000-14-05-1-0541.

[1] J. E. Bauerle, J. Phys. Chem. Solids **30**, 2657 (1969).
[2] X. Guo, W. Sigle, and J. Maier, J. Am. Ceram. Soc. **86**, 77 (2003).
[3] P. Jasinski, V. Petrovsky, T. Suzuki, and H. U. Anderson, J. Electrochem. Soc. **152**, J27 (2005).
[4] R. Andreaus and W. Sitte, J. Electrochem. Soc. **144**, 1040 (1997).
[5] W. Lai and S. M. Haile, J. Am. Ceram. Soc. **88**, 2979 (2005).
[6] S. B. Adler, Chem. Rev. (Washington, D.C.) **104**, 4791 (2004).
[7] Y. X. Lu, C. Kreller, and S. B. Adler, J. Electrochem. Soc. **156**, B513 (2009).
[8] N. J. Kidner, Z. J. Homrighaus, B. J. Ingram, T. O. Mason, and E. J. Garboczi, J. Electroceram. **14**, 283 (2005).
[9] N. J. Kidner, Z. J. Homrighaus, B. J. Ingram, T. O. Mason, and E. J. Garboczi, J. Electroceram. **14**, 293 (2005).
[10] Y. Nakao, Jpn. J. Appl. Phys., Part 1 **46**, 7008 (2007).
[11] N. J. Kidner, N. H. Perry, T. O. Mason, and E. J. Garboczi, J. Am. Ceram. Soc. **91**, 1733 (2008).
[12] J. H. Hwang, D. S. McLachlan, and T. O. Mason, J. Electroceram. **3**, 7 (1999).
[13] V. Petrovsky and F. Dogan, J. Am. Ceram. Soc. **92**, 1054 (2009).
[14] V. Petrovsky, T. Petrovsky, S. Kamlapurkar, and F. Dogan, J. Am. Ceram.

Soc. **91**, 3590 (2008).
[15]V. Petrovsky, T. Petrovsky, S. Kamlapurkar, and F. Dogan, J. Am. Ceram. Soc. **91**, 1814 (2008).
[16]V. Petrovsky, T. Petrovsky, S. Kamlapurkar, and F. Dogan, J. Am. Ceram. Soc. **91**, 1817 (2008).
[17]V. Petrovsky, A. Manohar, and F. Dogan, J. Appl. Phys. **100**, 014102 (2006).
[18]D. S. McLachlan, J. H. Hwang, and T. O. Mason, J. Electroceram. **5**, 37 (2000).
[19]J. R. Macdonald, *Impedance Spectroscopy: Emphasizing Solid Materials and Systems*, 1st ed. (Wiley, New York, 1987).
[20]C. H. Hsu and F. Mansfeld, Corrosion (Houston) **57**, 747 (2001).
[21]N. Bonanos and E. Lilley, J. Phys. Chem. Solids **42**, 943 (1981).
[22]M. L. Mansfield, J. F. Douglas, and E. J. Garboczi, Phys. Rev. E **64**, 061401 (2001).
[23]J. F. Douglas and E. J. Garboczi, Adv. Chem. Phys. **91**, 85 (1995).